

# Fine-tuning the Local Symmetry to Attain Record Blocking Temperature and Magnetic Remanence in a Single-Ion Magnet\*\*

Liviu Ungur, Jennifer J. Le Roy, Ilia Korobkov, Muralee Murugesu,\* and Liviu F. Chibotaru\*

Dedicated to Professor Marius Andruh on the occasion of his 60th birthday

**Abstract:** Remanence and coercivity are the basic characteristics of permanent magnets. They are also tightly correlated with the existence of long relaxation times of magnetization in a number of molecular complexes, called accordingly single-molecule magnets (SMMs). Up to now, hysteresis loops with large coercive fields have only been observed in polynuclear metal complexes and metal-radical SMMs. On the contrary, mononuclear complexes, called single-ion magnets (SIM), have shown hysteresis loops of butterfly/phonon bottleneck type, with negligible coercivity, and therefore with much shorter relaxation times of magnetization. A mononuclear  $\text{Er}^{\text{III}}$  complex is presented with hysteresis loops having large coercive fields, achieving 7000 Oe at  $T=1.8\text{ K}$  and field variation as slow as 1 h for the entire cycle. The coercivity persists up to about 5 K, while the hysteresis loops persist to 12 K. Our finding shows that SIMs can be as efficient as polynuclear SMMs, thus opening new perspectives for their applications.

The capacity of blocking the magnetization for a relatively long time makes single-molecule magnets (SMMs) prospective candidates for applications in information storage and processing technologies.<sup>[1–4]</sup> In the preceding years, a wide search for suitable compounds has been undertaken, ranging from magnetic networks,<sup>[5–7]</sup> mono-dimensional single-chain magnets,<sup>[8,9]</sup> polynuclear metal complexes,<sup>[10–14]</sup> metal-radical SMMs,<sup>[15]</sup> to molecules including one single magnetic ion. The latter class of molecules is heavily dominated by lanthanide-based single-ion magnets (SIMs),<sup>[16–21]</sup> although recently several mononuclear actinide-based<sup>[22,23]</sup> and transition metal-based<sup>[24]</sup> compounds were reported to show slow magnetic relaxation. Understanding the reasons and conditions necessary for the magnetic moment of individual ions or

molecules to be blocked as efficient as possible, that is, so that the additional energy required by the molecule for the reorientation of the magnetic moment to be as large as possible, is very important for designing efficient magnetic memory units, and great effort towards achieving this goal is being currently undertaken. To show blocking of magnetization at temperatures on the order of several Kelvin, the ground electronic multiplet of a complex should possess strong axial anisotropy and be separated from less anisotropic excited multiplets by at least few tens of wavenumbers. In the case of polynuclear SMMs, the strong exchange coupling between magnetic ions enhances the magnetization blocking. Achieving a strong exchange coupling regime between strongly anisotropic metal ions is not an easy task. In the cases of weak coupling, at temperatures higher than exchange splitting, the neighboring metal ions are sources of perturbing field, causing fast magnetic relaxation of polynuclear SMMs.<sup>[25]</sup>

On the other hand, the magnetic moment of single-magnetic ions becomes blocked as a result of strong spin-orbit coupling of the metal site and axial nature of the ligand environment. A high degree of axiality of the ligand field can be achieved in several ways in complexes lacking any strict site symmetry. One way is to achieve only one very short chemical bond with the metal ion, which favors significant orbital overlap between the electronic clouds of the ligating atom and the metal. This strong chemical bond dominates over all other chemical bonds of the metal site, leading to the intrinsically axial nature of the total ligand field felt by the metal ion. This effect has been predicted for  $\text{DyO}^+$  cation<sup>[26]</sup> and has been seen in the case of individual Dy ions in  $\text{Dy}_4\text{K}_2$  SMMs.<sup>[27]</sup> Another chemical route for obtaining an axial ligand field is to employ highly symmetrical ligands with no bonding atoms on the symmetry axis.<sup>[16]</sup> Accordingly, the first SIM reported by Ishikawa and co-workers<sup>[16]</sup> was a terbium phthalocyanine compound,  $(\text{Bu}_4\text{N})[\text{Tb}(\text{Pc})_2]$ , in which the  $\text{Tb}^{\text{III}}$  ion was sandwiched between two phthalocyanine ligands resulting in a symmetry close to  $D_{4d}$ . Should the symmetry be indeed so high, according to strict group-theoretical rules,<sup>[26]</sup> this complex as well as many similar ones, for example, with  $\text{Ln} = \text{Dy}^{\text{III}}, \text{Er}^{\text{III}}$ , would have been perfectly axial, that is, with completely suppressed quantum tunneling of magnetization (QTM) in the ground state. At the same time, gradual deviations from ideal symmetry result in the diminishing of axiality which induces increased QTM.<sup>[28]</sup> As an example, the  $[\text{Dy}(\text{Pc})_2]^-$  complex, isostructural with the described Tb isomer,<sup>[16]</sup> exhibits blocking of magnetization at the time scale of AC susceptibility measurement,<sup>[29]</sup> while the  $[\text{Dy}-$

[\*] Dr. L. Ungur, Prof. L. F. Chibotaru  
Theory of Nanomaterials Group and INPAC-Institute of Nanoscale Physics and Chemistry, Katholieke Universiteit Leuven  
Celestijnenlaan 200F, 3001 Leuven (Belgium)  
E-mail: Liviu.Chibotaru@chem.kuleuven.be

J. J. Le Roy, Dr. I. Korobkov, Prof. M. Murugesu  
Department of Chemistry, University of Ottawa  
10 Marie Curie, Ottawa, ON, K1N 6N5 (Canada)  
E-mail: M.Murugesu@uottawa.ca

[\*\*] L.U. is a post-doc of the Flemish Science Foundation (FWO-Vlaanderen) and also acknowledges the support from the INPAC and Methusalem programs of the KU Leuven. M.M. thanks the University of Ottawa, NSERC, CFI, ORF, and ERA.

Supporting information for this article is available on the WWW under <http://dx.doi.org/10.1002/ange.201310451>.

(SiW<sub>11</sub>O<sub>39</sub>)<sub>2</sub>]<sup>13-</sup> complex, showing larger deviations from an ideal *D*<sub>4d</sub> symmetry, exhibits slowing down of magnetic moment reversal but not its blocking in the same experiments.<sup>[18]</sup> Clearly higher SIM performance could be achieved by the use of ligands with higher rotational symmetry, such as planar cyclooctatetraene (COT) systems.<sup>[19,20,30,31]</sup> Indeed, recent ab initio calculations have predicted that an [Er(COT<sub>2</sub>)]<sup>-</sup> complex should be a high-performance SIM.<sup>[30]</sup>

With this in mind, our efforts focused on employment of highly symmetrical dianionic COT<sup>2-</sup> rings as ligands. The synthetic strategy for [Er(COT<sub>2</sub>)<sub>2</sub>]<sup>-</sup> and [Dy(COT<sub>2</sub>)<sub>2</sub>]<sup>-</sup> complexes was inspired by the latter reports where the appropriate Ln<sup>III</sup>Cl<sub>3</sub> is reacted with a COT dianion (K<sub>2</sub>COT) in an inert atmosphere with rigorous exclusion of air and water. Single crystals of [Er(COT<sub>2</sub>)<sub>2</sub>]<sup>-</sup> and [Dy(COT<sub>2</sub>)<sub>2</sub>]<sup>-</sup> were obtained following the addition of excess crown ether (18-crown-6). X-ray diffraction analyses reveal the two [K(18-crown-6)][Ln(COT<sub>2</sub>)<sub>2</sub>], Ln = Er<sup>III</sup>, Dy<sup>III</sup> complexes crystallize in an orthorhombic *P*<sub>nma</sub> space group. Full synthetic and structural details are provided in the Supporting Information. Figure 1 shows the X-ray structure of the magnetic anions [Er(COT<sub>2</sub>)<sub>2</sub>]<sup>-</sup> and [Dy(COT<sub>2</sub>)<sub>2</sub>]<sup>-</sup>. The structure is composed of two COT<sup>2-</sup> ligands bound in an η<sup>8</sup> fashion to the central Ln<sup>III</sup>

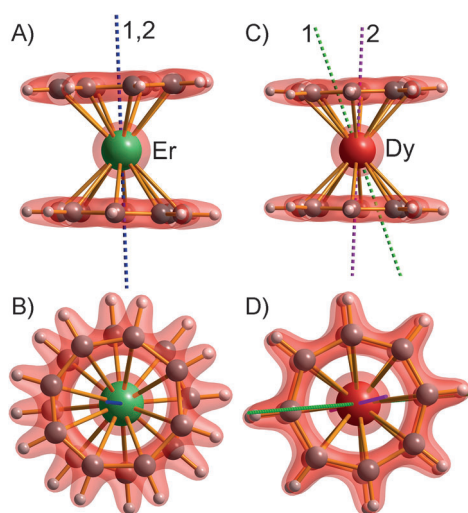


**Figure 1.** Molecular structure of [Ln<sup>III</sup>(COT<sub>2</sub>)<sub>2</sub>]<sup>-</sup> magnetic anions. A) side and B) top view for Ln = Er; C) side and D) top view for Ln = Dy. The [K(18-crown-6)]<sup>+</sup> cation, which is coordinated to one of the COT rings, is not shown for clarity. Er green, Dy red, C gray, H white. Distance between centers of COT rings: 3.74 Å (Er); 3.81 Å (Dy); mean eccentricity of COT rings is small: 0.11 (Er) and 0.21 (Dy); shortest distance between two neighboring molecules in the crystal is 7.25 Å (Er); 7.09 Å (Dy). The transparent red surface shows the calculated electronic density in the ground state. Note the higher rotational symmetry of the electronic cloud close to the Ln ion than expected from an octagonal group. Dashed lines show the calculated orientation of the main magnetic axis on Ln ions in the ground (1) and first excited (2) Kramers doublet. For Er:  $g_{x,y} = 3.5 \times 10^{-6}$ ,  $g_z = 17.96$  for the ground doublet and  $g_{x,y} = 5.4 \times 10^{-4}$ ,  $g_z = 15.53$  for the first excited doublet; the angle between corresponding  $g_z$  axes is about 1.0°. For Dy:  $g_{x,y} = 1.6 \times 10^{-1}$ ,  $g_z = 12.64$  for the ground doublet (green dashed line) and  $g_{x,y} = 5.8 \times 10^{-2}$ ,  $g_z = 13.84$  for the first excited doublet (purple dashed line); the angle between corresponding  $g_z$  axes is about 21°.

ion, and a counterion composed of one equivalent of [K(18-crown-6)]. In both complexes, the K counterion asymmetrically interacts with the COT ring, ((K–C<sub>COT</sub> distances between 3.25(8)–3.39(3) Å (Er), and 3.29(9)–3.81(7) Å (Dy)), which is considered to be weak K–C interactions. The near-linear structure is reflected in COT<sub>centroid</sub>–Ln<sup>III</sup>–COT<sub>centroid</sub> angle, which deviates from perfect linearity (180°) by 1.96° (Er) and 6.15° (Dy). However a distinct tilt angle (3.57° (Er) and 2.4° (Dy)) as well as non-equivalent ligand donation from each COT ring (Ln–COT<sub>centroid</sub> distances (1.85(2) Å, 1.89(1) Å (Er); 1.89(3) Å, 1.91(8) Å (Dy)) are a result of the interacting counterion. The eightfold symmetry axis of the COT groups and their parallel arrangement preserve the high symmetry axis in both complexes. Besides, the Er complex is close to a *D*<sub>8d</sub> symmetry, while the Dy compound is more eclipsed, being closer to *D*<sub>8h</sub>. In both complexes, the axial symmetry is higher than in previously synthesized SIMs,<sup>[16–21]</sup> therefore, we believe higher magnetic blocking performance can be achieved through our molecular approach.

In contrast to the structural similarity of these complexes, their magnetic behavior exhibits strong divergence. Figure 2 shows measured out-of-phase ( $\chi''$ ) ac magnetic susceptibility for both compounds. The Er complex exhibits indeed a very

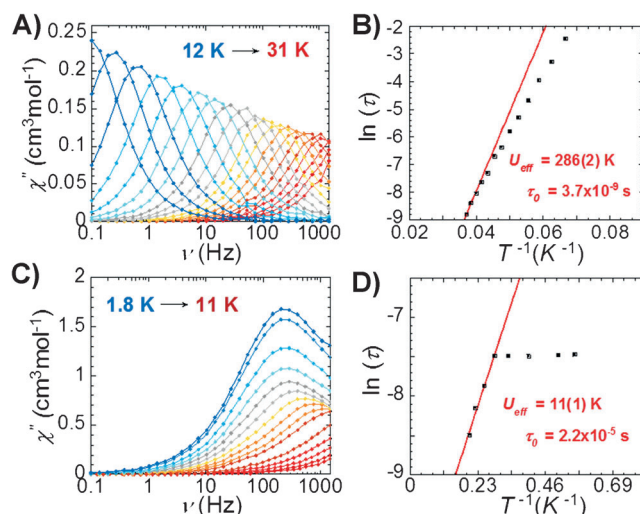


**Figure 2.** Dynamic magnetic susceptibility. Out-of-phase component  $\chi''$  for Er (A) and Dy (C) compounds measured in the frequency range 0.1 Hz–1.5 kHz, in zero DC field and at indicated temperatures; Arrhenius treatment of  $\chi''$  data for Er (B) and Dy (D), with the solid red line indicating the fit of the data. Note that below 12 K, the reversal of magnetization in the Er compound takes more than 10 s, which prevents extraction of relaxation times in the low-temperature region. The extracted blocking barriers are in good agreement with the calculated positions of the corresponding excited states through which the temperature-assisted (TA) magnetic relaxation occurs at high temperatures (Figure 4; Supporting Information, Tables S2, S6).

strong blocking of magnetization precluding the extraction of the relaxation times for temperatures lower than 12 K (Figure 2B) between 0.1–1500 Hz, a phenomenon not observed in other SIM complexes. Surprisingly enough the Dy complex shows much weaker magnetization blocking, with relaxation times many orders of magnitude lower than in

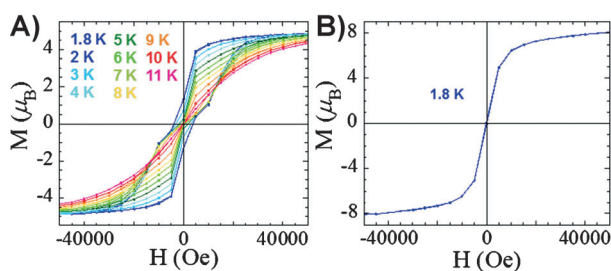


**Figure 3.** Magnetization hysteresis loops. A)  $M$  vs.  $H$  for  $[\text{Er}(\text{COT})_2]^-$  measured on a SQUID at  $35 \text{ Oe s}^{-1}$  sweep rate and at indicated temperatures. At  $T = 1.8 \text{ K}$  the coercivity (distance between  $M(H)$  points at  $M = 0$ ) is about  $7000 \text{ Oe}$ . B) Equivalent measurement for  $[\text{Dy}(\text{COT})_2]^-$  at  $1.8 \text{ K}$ .

the Er compound (Figure 2D), despite its close structure with the latter (Figure 1).

Figure 3 shows the magnetization loops for powdered crystalline samples of  $[\text{Er}(\text{COT})_2]^-$  and  $[\text{Dy}(\text{COT})_2]^-$ . The remarkably high blocking temperature observed for the Er analogue is reflected by the large coercive field (ca.  $7000 \text{ Oe}$  at  $1.8 \text{ K}$ ), a feature not seen before for mononuclear transition metal or lanthanide SIM.<sup>[16–21,29]</sup> Indeed, in all of the previously reported SIM complexes, a negligible value of the coercive field was detected at much lower temperatures, usually below  $0.1 \text{ K}$ . It originates most probably from the coupling between the electronic magnetic moment and the nuclear spin of the metal ion. In the present case, the reported coercive field is due to the blockage of the electronic magnetic moment itself. The observed large coercive field for the Er compound is in good agreement with the AC susceptibility measurements (Figure 2A,B), from which relaxation times of seconds and tens of seconds can be inferred at  $T < 12 \text{ K}$ . On the other hand, the fast magnetic relaxation of the Dy compound seen in AC measurements in Figure 2C,D prevents the appearance of magnetic hysteresis (Figure 3B).

Ab initio CASSCF/RASSI/SINGLE\_ANISO calculations with MOLCAS 7.8<sup>[32]</sup> predict the ground state of the Er compound is well separated from the low-lying excited states, strong magnetic anisotropy of the ground ( $g_{x,y} \approx 10^{-6}$ ) and of the first excited Kramers doublet, with almost collinear anisotropy axes (Figures 1A,B and 4; Supporting Information, Tables S2, S3, S5). On the other hand, calculations predict much denser low-lying energy spectrum for the Dy compound, lower degree of magnetic axiality in the lowest Kramers doublet ( $g_{x,y} \approx 10^{-1}$ ), non-collinear anisotropies of ground and excited states (Figure 1C,D; Tables S6, S7, S9).

Similar ab initio calculations on symmetrized models of the Er compound with  $C_8$  point group revealed an energy spectrum almost independent of the relative angular positions of the COT rings, assumed parallel to each other (Supporting Information, Figure S7). This confirms that the central  $\text{Ln}^{\text{III}}$  ion feels indeed an almost perfectly rotational (that is, described by a symmetry axis of infinite order) electronic density from a ring, a conclusion already anticipated from Figure 1. Studies concerning the effect of the Ln-COT distance on the low-lying electronic spectrum (Supporting Information, Figure S8) revealed a large domain of R(Ln-

COT) for which the properties of the ground and of the few excited states reported above are similar.

As found previously, the strengths of QTM and the rate of spin-phonon transitions are loosely proportional to the square of the transversal magnetic moment connecting the magnetic states of the complex.<sup>[33,34]</sup> The blocking barrier can be defined, therefore, by the shortest paths where the values of the transversal magnetic moment are the largest.<sup>[35]</sup> Figure 4 shows ab initio constructed magnetization blocking barriers for Er and Dy compounds. For the former we notice the negligible value of the transversal magnetic moment in the ground state (ca.  $10^{-6} \mu_B$ ), which explains why the QTM is suppressed at low temperature in this compound. The transversal magnetic moment is small for the first excited state either (ca.  $10^{-4} \mu_B$ ), therefore, thermally assisted QTM will be quenched for this Kramers doublet as well. Owing to the collinearity of anisotropy axes of the ground and first excited Kramers doublets, the off-diagonal matrix element of the transversal magnetic moment between their components of opposite magnetization is also small (ca.  $10^{-5} \mu_B$ ) and the corresponding Orbach process is suppressed. As a result, magnetic relaxation in the Er compound can only occur by the second excited state, which allows significant thermally-assisted tunneling (Figure 4a). This effect was recently found to increase significantly the height of blocking barriers in lanthanide SMMs.<sup>[27]</sup> In contrast, the Dy compound has significantly larger value of the transversal magnetic moment already in the ground state (ca.  $10^{-1} \mu_B$ ), therefore allowing a fast QTM. Moreover, the tunneling in the excited state is also allowed (ca.  $10^{-1} \mu_B$ ), enhancing overall the reversal of magnetization at higher temperatures.

To understand the ultimate reason for the high SIM performance of the Er compound compared to the Dy compound, we calculated the parameters of the multiplet-specific crystal field for these compounds on the basis of ab initio wavefunctions and energies (Supporting Information, Tables S10, S11). We found that the axial parameters  $B_2^0$ ,  $B_4^0$ ,  $B_6^0$  are by far the largest, while the non-axial parameters are one or more orders of magnitude smaller. The wavefunction of the ground state of Er compound is almost of pure  $\pm 15/2$  type, with negligible contributions from other  $J$ -projections (weight  $< 10^{-4}$ ). In contrast, the wavefunction of the ground state of the Dy compound is of  $\pm 9/2$  type, with significantly larger contributions from other  $J$ -projections (with a weighting of about 4.5%). This is explained by a much larger energy gap between the ground and first excited Kramers doublet in  $[\text{Er}(\text{COT})_2]^-$  compound compared to  $[\text{Dy}(\text{COT})_2]^-$ . Such a large difference between the energy gaps originates from the fact that the most important crystal-field parameters  $B_2^0$  and  $B_4^0$  have opposite signs for Er and Dy (because the corresponding Stevens parameters  $\alpha$  and  $\beta$  have opposite signs for the ground  $J = 15/2$ ),<sup>[36]</sup> which is confirmed in ab initio calculations (Supporting Information, Tables S10, S11). For this reason, the spectra of Er and Dy compounds look as being mutually reversed. Indeed, the highest excited Kramers doublet for Dy is obtained very axial and of  $\pm 15/2$  type (Figure 4; Supporting Information, Tables S6, S7).

The ultimate reason for the easy axis behavior of the Er complex is the negative sign of the dominant  $B_2^0$  parameter

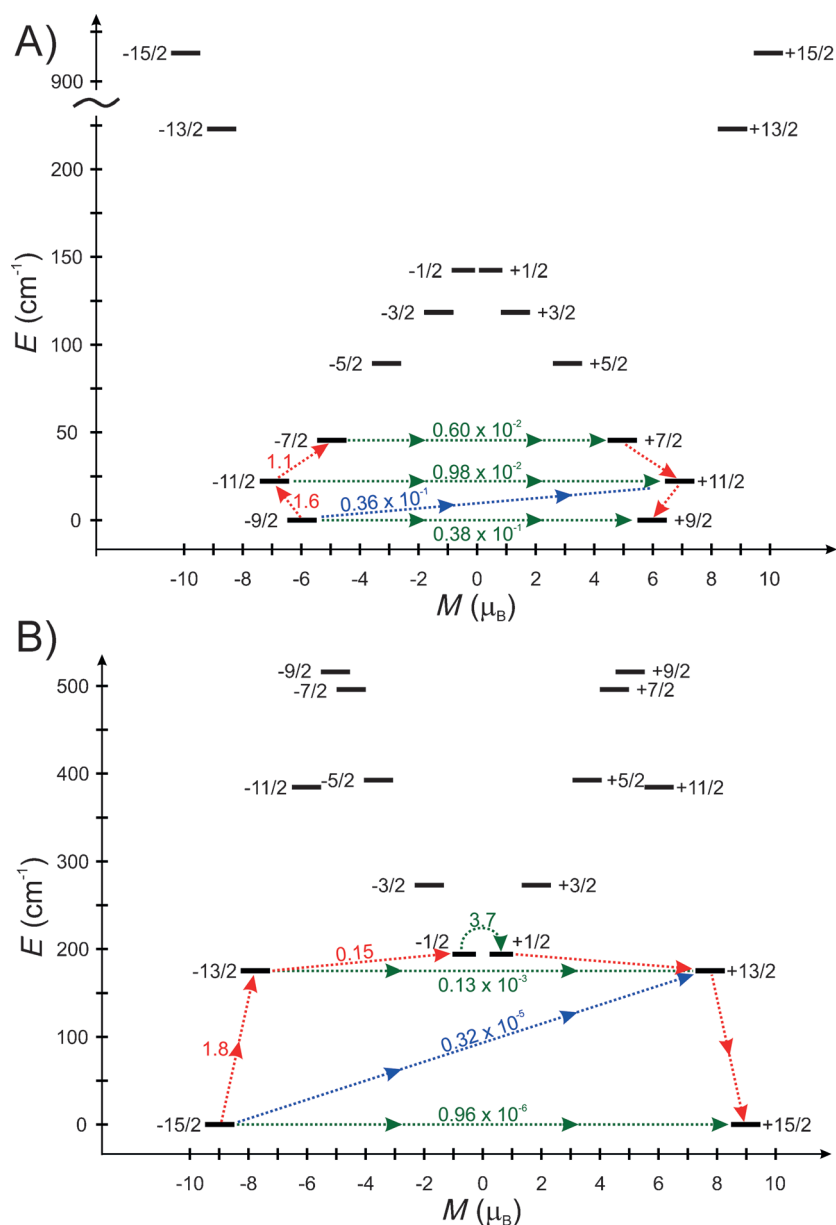


**Figure 4.** The magnetization blocking barriers in Dy (A) and Er (B) compounds. The thick black lines represent the Kramers doublets as a function of their magnetic moment along the axis connecting the centers of COT rings. The green dashed lines correspond to diagonal quantum tunneling of magnetization (QTM); the blue dashed lines represent Orbach relaxation processes. The numbers at each arrow stand for the mean absolute value of the corresponding matrix element of transition magnetic moment ( $(|\mu_x| + |\mu_y| + |\mu_z|)/3$ ). The path shown by the red arrows represents the most probable path for magnetic relaxation in the corresponding compounds.

(Supporting Information, Table S10). On the other hand, the non-monotonic behavior of the Stevens operator  $O_4^0$  on  $J_z^2$ , corresponding next largest parameter  $B_4^0$ , is the reason why the  $\pm 1/2$  is not the ground state, that is, why Dy is not of pure easy plane type (Figure 4A).

In conclusion, the exceptional magnetic properties of the reported single-ion magnet (SIM) complex containing one  $\text{Er}^{\text{III}}$  ion sandwiched between two planar COT ligands (the

large coercive field up to 7000 Oe at 1.8 K and magnetic remanence up to 6 K) makes the reported compound comparable to polynuclear single-molecule magnets (SMM). The present study for the first time brings the entire family of SIM compounds to the class of permanent magnets. Besides showing unprecedented capability for magnetization blocking, the present Er complex certainly possess the ability to be uniformly attached by  $\pi$ - $\pi$  stacking to various surfaces such as graphene or metal surfaces. This opens the way to employ the present Er compound in spintronics<sup>[37,38]</sup> and other applications, such as information storage, requiring a significant magnetic blocking capacity at helium temperatures.<sup>[39,40]</sup>

### Experimental Section

The ab initio calculations of electronic spectra magnetic properties, Zeeman tensors, and crystal-field parameters of the compounds have been done with MOLCAS package and the Single\_Aniso routine as described elsewhere (see the Supporting Information for the details).

All syntheses were performed under inert atmosphere glove box as both complexes are extremely air- and moisture-sensitive. Isolated single crystals were analyzed with a Bruker-AXS SMART 1 k CCD diffractometer, NMR spectroscopy, and elemental analysis. Magnetic characterizations were carried out using a Quantum Design SQUID magnetometer MPMS-XL7 operating between 1.8 and 300 K for applied DC fields ranging from  $-7$  to  $7$  T. Specific details on synthesis and characterization can be found in the Supporting Information.<sup>[41]</sup>

Received: December 2, 2013

Revised: January 6, 2014

Published online: March 20, 2014

**Keywords:** lanthanides · magnetic hysteresis · magnetic remanence · quantum chemistry · single-molecule magnets

[1] D. Gatteschi, R. Sessoli, J. Villain, *Molecular Nanomagnets*, Oxford University Press, New York, 2006.

[2] R. Sessoli, D. Gatteschi, A. Caneschi, M. A. Novak, *Nature* **1993**, 365, 141–143.

[3] L. Bogani, W. Wernsdorfer, *Nat. Mater.* **2008**, 7, 179–186.

[4] M. N. Leuenberger, D. Loss, *Nature* **2001**, 410, 789–793.

[5] S. Ferlay, T. Mallah, R. Ouahes, P. Veillet, M. Verdaguer, *Nature* **1995**, 378, 701–703.

[6] K. Fegy, D. Luneau, T. Ohm, C. Paulsen, P. Rey, *Angew. Chem.* **1998**, 110, 1331–1335; *Angew. Chem. Int. Ed.* **1998**, 37, 1270–1273.



- [7] H. Miyasaka, K. Nakata, L. Lecren, C. Coulon, Y. Nakazawa, T. Fujisaki, K. Sugiura, M. Yamashita, R. Clerac, *J. Am. Chem. Soc.* **2006**, *128*, 3770–3783.
- [8] R. Cl  rac, H. Miyasaka, M. Yamashita, C. Coulon, *J. Am. Chem. Soc.* **2002**, *124*, 12837–12844.
- [9] H. Miyasaka, M. Julve, M. Yamashita, R. Clerac, *Inorg. Chem.* **2009**, *48*, 3420–3437.
- [10] J. R. Friedman, M. P. Sarachik, J. Tejada, R. Ziolo, *Phys. Rev. Lett.* **1996**, *76*, 3830.
- [11] L. Thomas, F. Lionti, R. Ballou, D. Gatteschi, R. Sessoli, B. Barbara, *Nature* **1996**, *383*, 145–147.
- [12] W. Wernsdorfer, T. Ohm, C. Sangregorio, R. Sessoli, D. Mailly, C. Paulsen, *Phys. Rev. Lett.* **1999**, *82*, 3903.
- [13] D. N. Woodruff, R. E. P. Winpenny, R. A. Layfield, *Chem. Rev.* **2013**, *113*, 5110–5148.
- [14] R. Sessoli, A. K. Powell, *Coord. Chem. Rev.* **2009**, *253*, 2328–2341.
- [15] J. D. Rinehart, M. Fang, W. J. Evans, J. R. Long, *Nat. Chem.* **2011**, *3*, 538–542.
- [16] N. Ishikawa, M. Sugita, T. Ishikawa, S. Koshihara, Y. Kaizu, *J. Am. Chem. Soc.* **2003**, *125*, 8694–8695.
- [17] S. Takamatsu, T. Ishikawa, S. Koshihara, N. Ishikawa, *Inorg. Chem.* **2007**, *46*, 7250–7252.
- [18] M. A. AlDamen, S. Cardona-Serra, J. M. Clemente-Juan, E. Coronado, A. Gaita-Ari  o, C. Mart  -Gastaldo, F. Luis, O. Montero, *Inorg. Chem.* **2009**, *48*, 3467–3479.
- [19] S.-D. Jiang, S.-S. Liu, L.-N. Zhou, B.-W. Wang, Z.-M. Wang, S. Gao, *Inorg. Chem.* **2012**, *51*, 3079–3087.
- [20] S.-D. Jiang, B.-W. Wang, H.-L. Sun, Z.-M. Wang, S. Gao, *J. Am. Chem. Soc.* **2011**, *133*, 4730–4733.
- [21] G. Cucinotta, M. Perfetti, J. Luzon, M. Etienne, P.-E. Car, A. Caneschi, G. Calvez, K. Bernot, R. Sessoli, *Angew. Chem.* **2012**, *124*, 1638–1642; *Angew. Chem. Int. Ed.* **2012**, *51*, 1606–1610.
- [22] M. A. Antunes, L. C. J. Pereira, I. C. Santos, M. Mazzanti, J. Mar  o, M. Almeida, *Inorg. Chem.* **2011**, *50*, 9915–9917.
- [23] N. Magnani, C. Apostolidis, A. Morgenstern, E. Colineau, J.-C. Griveau, H. Bolvin, O. Walter, R. Caciuffo, *Angew. Chem.* **2011**, *123*, 1734–1736; *Angew. Chem. Int. Ed.* **2011**, *50*, 1696–1698.
- [24] J. M. Zadrozny, D. J. Xiao, M. Atanasov, G. J. Long, F. Grandjean, F. Neese, J. R. Long, *Nat. Chem.* **2013**, *5*, 577–581.
- [25] A. Bhunia, M. T. Gamer, L. Ungur, L. F. Chibotaru, A. K. Powell, Y. Lan, P. W. Roesky, F. Menges, C. Riehn, G. Niedner-Schatteburg, *Inorg. Chem.* **2012**, *51*, 9589–9597.
- [26] L. Ungur, L. F. Chibotaru, *Phys. Chem. Chem. Phys.* **2011**, *13*, 20086–20090.
- [27] R. J. Blagg, L. Ungur, F. Tuna, J. Speak, P. Comar, D. Collison, W. Wernsdorfer, E. J. L. McInnes, L. F. Chibotaru, R. E. P. Winpenny, *Nat. Chem.* **2013**, *5*, 673–678.
- [28] H. L. C. Feltham, Y. Lan, F. Kl  wer, L. Ungur, L. F. Chibotaru, A. K. Powell, S. Brooker, *Chem. Eur. J.* **2011**, *17*, 4362–4365.
- [29] N. Ishikawa, M. Sugita, T. Ishikawa, S. Koshihara, Y. Kaizu, *J. Phys. Chem. B* **2004**, *108*, 11265–11271.
- [30] J. J. Le Roy, M. Jeletic, S. I. Gorelsky, I. Korobkov, L. Ungur, L. F. Chibotaru, M. Murugesu, *J. Am. Chem. Soc.* **2013**, *135*, 3502–3510.
- [31] M. Jeletic, P.-H. Lin, J. J. Le Roy, I. Korobkov, S. I. Gorelsky, M. Murugesu, *J. Am. Chem. Soc.* **2011**, *133*, 19286–19289.
- [32] F. Aquilante, L. De Vico, N. Ferre, G. Ghigo, P. A. Malmqvist, P. Neogrady, T. B. Pedersen, M. Pitonak, M. Reiher, B. O. Roos, L. Serrano-Andres, M. Urban, V. Veryazov, R. Lindh, *J. Comput. Chem.* **2010**, *31*, 224–247; <http://www.molcas.org>.
- [33] D. A. Garanin, E. M. Chudnovsky, *Phys. Rev. B* **1997**, *56*, 11102–11118.
- [34] M. N. Leuenberger, D. Loss, *Phys. Rev. B* **2000**, *61*, 1286.
- [35] L. Ungur, M. Thewissen, J. P. Costes, W. Wernsdorfer, L. F. Chibotaru, *Inorg. Chem.* **2013**, *52*, 6328–6337.
- [36] A. Abragam, B. Bleaney, *EPR of Transition Ions*, Oxford University Press, Oxford, **1970**, Table 20.
- [37] K. Katoh, H. Isshiki, T. Komeda, M. Yamashita, *Chem. Asian J.* **2012**, *7*, 1154–1169.
- [38] S. A. Wolf, D. D. Awschalom, R. A. Buhrman, J. M. Daughton, S. von Molnar, M. L. Roukes, A. Y. Chtchelkanova, D. M. Treger, *Science* **2001**, *294*, 1488–1495.
- [39] R. Vincent, S. Klyatskaya, M. Ruben, W. Wernsdorfer, F. Balestro, *Nature* **2012**, *488*, 357–360.
- [40] M. Mannini, F. Pineider, P. Saintavrit, C. Danieli, E. Otero, C. Sciancalepore, A. M. Talarico, M. A. Arrio, A. Cornia, D. Gatteschi, R. Sessoli, *Nat. Mater.* **2009**, *8*, 194–197.
- [41] Note added in proof (March 15, 2014): After submitting this article we learned that another publication containing the experimental investigation of similar Er compound has recently appeared: K. R. Meihaus, J. R. Long, *J. Am. Chem. Soc.* **2013**, *135*, 17952–17957.